energy&fuels

pubs.acs.org/EF

Article

Experimental Investigation of Critical Parameters Controlling CH_4–CO_2 Exchange in Sedimentary CH_4 Hydrates

Stian Almenningen,* Arne Graue, and Geir Ersland

Cite This: *Energy Fuels* 2021, 35, 2468–2477

Read Online

ACCESS | Metrics & More | Article Recommendations

ABSTRACT: Sequestration of CO_2 in natural gas hydrate reservoirs may offer stable long-term deposition of a greenhouse gas while benefiting from CH_4 gas production. In this paper, we review old and present new experimental studies of CH_4–CO_2 exchange in CH_4 hydrate-bearing sandstone core plugs. CH_4 hydrate was formed in Bentheim sandstone core plugs to prepare for subsequent lab-scale CH_4 gas production by CO_2 replacement. The effect of temperature, diffusion length, salinity, water saturation, CH_4 hydrate saturation, and co-injection of chemicals (N_2 and monoethanolamine) with the injected CO_2 were measured. The measurements prove the critical role of water saturation in these processes: formation of CO_2 hydrate severely reduced the injectivity for water saturations above 0.1 fractions. The results presented in this paper are important when assessing natural gas hydrate reservoirs as candidates for CO_2 injection with concurrent CH_4 gas production.

1. INTRODUCTION

Natural gas hydrates are solid crystalline inclusion compounds with the ability to encapsulate guest molecules in structural cages of water molecules at moderate to high pressure and low temperature. Estimates of natural gas volumes trapped in gas hydrates range between 10^{14} and 10^{18} Sm^3, where the high-end estimate compares to known reserves of conventional fossil energy resources.[1] The environmental advantage with methane (CH_4) gas, compared to oil and coal, is that it burns cleaner upon combustion and release less carbon dioxide (CO_2) to the atmosphere per unit energy. Production of CH_4 gas by depressurization is the most tested method at the field scale.[2−4] However, injection of CO_2 to provide a thermodynamically more stable gas hydrate compared to the native CH_4 hydrate is also a tested scheme of production.[5] Several experiments have shown that exposing CH_4 hydrates to CO_2 leads to a spontaneous exchange of molecules in which the large cavities of structure I hydrates prefer occupation by CO_2.[6−9] The exchange process is driven by kinetics and the exothermic nature of CO_2 hydrate formation. The released heat through CO_2 hydrate formation (−57.98 kJ/mol) is higher than the heat required for CH_4 hydrate dissociation (54.49 kJ/mol), which may accelerate the exchange process.[10] The increased thermodynamic stability will keep the gas hydrate in the solid state and maintain the structural integrity of the sediments.[11,12] In sum, injection of CO_2 in hydrates poses two environmental advantages compared to pressure depletion: (1) geological sequestration of the greenhouse gas CO_2 and (2) lower risk of geomechanical instability.

There have been several studies to investigate the effectiveness of CO_2 injection with concurrent CH_4 gas production in CH_4 hydrates. However, the reported recovery rates of CH_4 gas are very scattered and reflect the variety of experimental procedures and conditions used.[13] Several studies involving continuous CO_2 injection into CH_4 hydrate-bearing sediments exist,[13−17] but none of them systematically address the effect of residual water saturation. The CH_4 hydrate-bearing sediments in nature must be permeable such that the injected CO_2 may penetrate deep into the formation and contact the CH_4 hydrate. This is challenging since the injected CO_2 easily forms CO_2 hydrates with the pore water at the prevailing pressure and temperature and the injectivity may be lost in the near-well region.[18] The main criterion for a successful injection of CO_2 in CH_4 hydrate deposits is to maintain injectivity during the injection and production stage. Adding nitrogen (N_2) to the injected CO_2 has thus been recognized as an effective technique to ensure injectivity and was implemented during the short-term CH_4–CO_2 exchange field trial on the Alaska North Slope in 2012.[5] Adding N_2 to the gas mixture increases the hydrate equilibrium pressure and promotes CH_4 gas recovery.[17,19] Other destabilizing chemicals such as hydrogen[20] and methanol[21] have also been tested in the laboratory as a mean to increase the recovery rate of CH_4 gas.

In this paper, we present a series of CO_2 injections into CH_4 hydrate-bearing sandstone cores with different liquid water saturations to delineate the water saturation transition where CO_2 injection becomes impractical. The results build on the work presented in Birkedal et al.[22] and include the effect of diffusion length, temperature, salinity, water saturation, and CH_4 hydrate saturation on CH_4–CO_2 exchange rates. The advantage of mixing CO_2 with N_2 and monoethanolamine

Received: November 13, 2020
Revised: January 6, 2021
Published: January 22, 2021

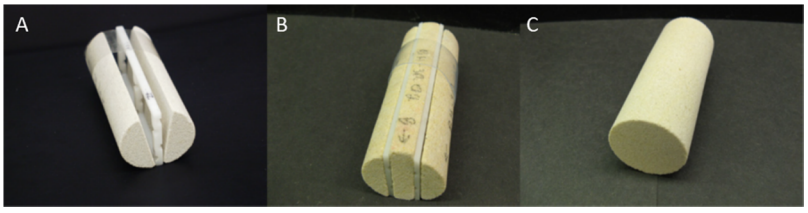

Figure 1. Core plug design of single fracture (A), double fracture (B), and unfractured (C) experiments. A POM spacer was placed in the fractures to maintain a constant fracture aperture during experiments. Reproduced from Birkedal et al.[22]

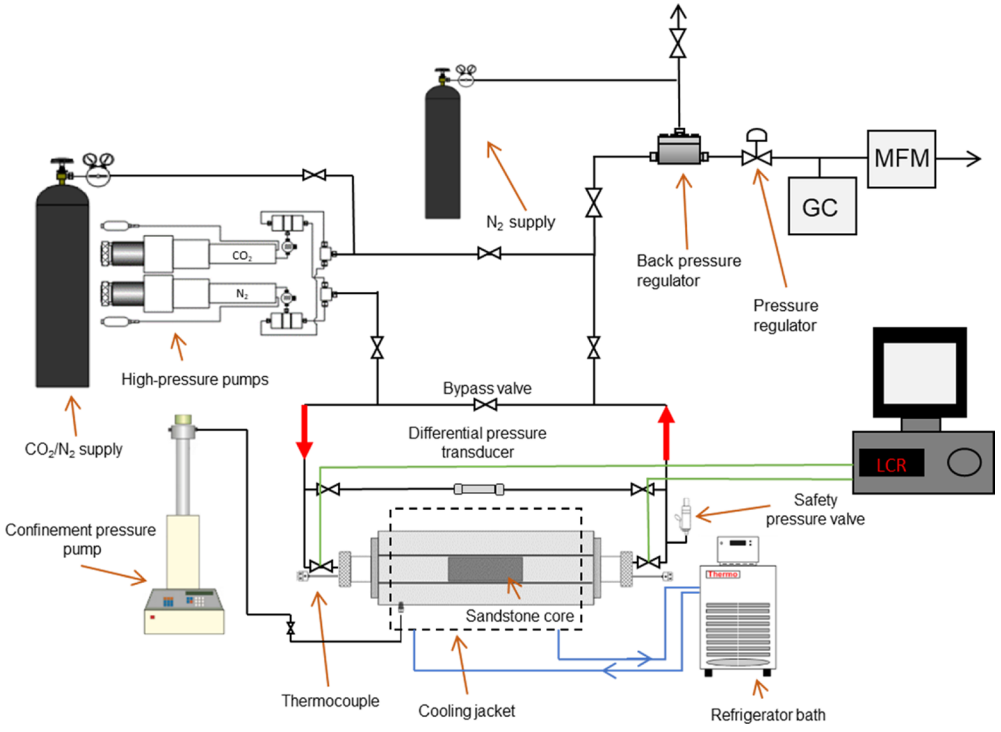

Figure 2. Experimental setup including differential pressure transducer, LCR meter, gas chromatograph, and mass flow meter. CO_2 was injected from left to right through whole core plugs saturated with CH_4 hydrate, water, and free CH_4 gas.

(MEA) is demonstrated in sediments containing CH_4 hydrate and elevated water saturations.

2. EXPERIMENTAL SECTION

2.1. Core Preparation. CH_4 hydrates were formed in the pore space of a high porosity, highly permeable sandstone acquired from the Bentheim quarry in Lower Saxony, Germany. The Bentheim sample used in these experiments had a porosity of 22−24% and a permeability of 1−2 D and was characterized by uniform pore geometry with an average pore diameter of 125 μm. The sand grains consisted of 95% quarts. Three core plug geometries were used in these experiments (Figure 1): The first (Figure 1A) was designed with an open fracture separated with a POM spacer down the long axis of the core plug.[6] The centered fracture divided the core plug in two half cylinders of equal size. The second core geometry (Figure 1B) contained two fractures that each was separated by a POM spacer. The double fracture arrangement increased the surface area of injected CO_2 toward the core plug and reduced the diffusion length of CO_2 into the CH_4 hydrate-saturated pores. The third design (Figure 1C) was unfractured whole cylindrical core plugs.

2.2. CH_4−CO_2 Exchange in Fractured Cores. The fractured cores (single or double fracture) were sealed with Teflon shrink tubing and placed inside a magnetic resonance imaging (MRI, superconducting Unity/Inova-Imaging 85/310 spectrometer) compatible high-pressure cell. The Teflon sleeve ensured that the pore fluids could flow through the core plug while the plug was separated from the confining fluid. Water with a given salinity was injected (Quizix C-6000) into the core plug before the plug was flushed with CH_4 gas to displace water from the fracture(s). CH_4 hydrate was formed by cooling the sample at a constant pore pressure of 8.3 MPa. The temperature was maintained at 4.0 ± 0.2 °C during weeks of operation. CH_4 hydrate formation was measured as a loss of MRI intensity as the liquid water converted to solid hydrates. A detailed description of the MR imaging technique can be found in Baldwin et al.[23] When the MR signal became constant and the phase transitions ceased, CO_2 was injected at a constant flow rate into the core plug and displaced the CH_4 gas from the fracture(s). The outlet valve was then closed, and the CO_2 pressure was kept constant at 8.3 MPa for several weeks. The CH_4−CO_2 exchange process was monitored with the MRI as CH_4 gas liberated from the CH_4 hydrate diffused back into the fracture(s). The MR signal of the CH_4 gas was used to quantify the molar concentration of CH_4 gas in the fracture(s) during the exchange process by comparing the MR signal to a baseline signal of 100% CH_4 gas in the fracture(s) at similar pressure, see Baldwin et al.[23] for details. After the increase of CH_4 concentration in the fracture(s) leveled off, a second CO_2 flush was conducted to supply pure CO_2 to the fracture(s) and thereby to increase the chemical potential of CO_2.

2.3. CH_4−CO_2 Exchange in Whole Cores. An experimental setup without MRI capabilities was used to perform CO_2 injections into whole core plugs (Figure 2). The core plugs were presaturated with water, mounted in a Hassler core holder, and pressurized with CH_4 gas to 8.3 MPa by a high-pressure pump (ST Stigma 1000). The

https://dx.doi.org/10.1021/acs.energyfuels.0c03841
Energy Fuels 2021, 35, 2468−2477

CH_4 hydrate formation started as the core plug was cooled to 4 °C by circulating antifreeze (Thermo Neslab RTE17) through a surrounding cooling jacket. The amount of consumed CH_4 gas was measured at constant pressure during the hydrate growth period and the formed hydrate volume was quantified as

$$V_{\text{hydrate}} = \left(\frac{\left(\frac{V_{\text{CH4}} \times \rho_{\text{CH4}}^{\text{pump}}}{Mm_{\text{CH4}}} \right) \times \upsilon \times Mm_{\text{w}}}{\rho_{\text{w}}^{\text{core}}} \right) \times 1.26 \quad (1)$$

where V_{CH4} is the consumed volume of CH_4 gas [mL], υ is the hydration number, ρ is the density [g/mL], and Mm is the molar mass [g/mole]. The last factor, 1.26, is the expansion of water as water molecules convert from liquid to hydrate form. The hydrate saturation was found by dividing the volume of hydrate by the pore volume. Subsequently, pure CO_2, or CO_2 mixed with N_2 or monoethanolamine (MEA), was injected in the core with a constant volumetric flow rate measured by a high-pressure pump. A range of critical parameters such as CH_4 hydrate saturations, water saturations, water salinities, and exchange temperatures were studied with respect to CH_4 gas recovery rates. The produced effluent was continuously sampled and analyzed using an inline gas chromatograph (Agilent 3000A) and a mass flow meter (Bronkhorst M13 Coriolis). The combination of these measurements gave produced amount (moles) of CH_4 gas as a function of time. The amount of produced CH_4 gas is presented relative to the total amount of hydrate-bound CH_4 gas and free CH_4 gas in the core plug prior to CO_2 injection. Hence, most of the results show the total CH_4 gas recovery: the produced fraction of free and hydrate-bound CH_4 gas.

3. RESULTS AND DISCUSSION

3.1. Diffusive CH_4–CO_2 Exchange in Fractured Cores.

Figure 3 shows a series of MRI images collected from a CH_4 hydrate-bearing core containing a single fracture after CO_2 was injected to displace CH_4 from the fracture. Similar experiments are previously reported by Birkedal et al.,[22] Ersland et al.,[24] and Graue et al.[6] The outlet valve was closed after the CO_2 flush, leaving the system isolated with a reservoir of liquid CO_2 holding constant pressure. CO_2 could then diffuse into the two core halves and CH_4 was produced back into the fracture over time. The first image (A) was acquired after the system was flushed with CO_2. The fracture with CO_2 appeared empty (no MRI signal) as CO_2 contains no hydrogen, suggesting that approximately all CH_4 in the fracture was displaced by CO_2 during the flush. The second image (B) was acquired 112 h after the flush, at which time the MRI signal reappeared in the fracture. Figure 3 C,D shows successive images obtained after 181 and 604 h, respectively, as the CH_4–CO_2 exchange reaction continuously provided CH_4 gas that diffused into the fracture.

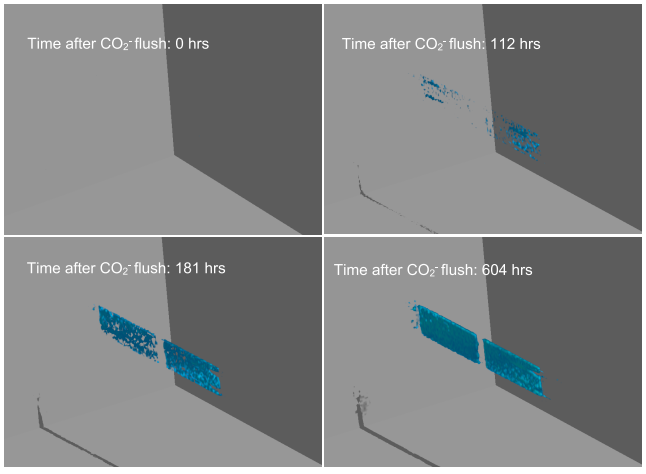

Figure 3. CH_4 gas produced by CO_2 replacement from a CH_4 hydrate-bearing core plug containing a fracture. The amount of CH_4 gas (blue signal) increases continuously in the fracture volume as the exchange reaction proceeds. The pore pressure and temperature were 8.3 MPa and 4 °C, respectively. Reproduced from Ersland et al.[25]

3.2. Effect of Diffusion Length and Surface Area.

The effect of increased surface area and decreased diffusion length on CH_4 gas recovery rates was studied by comparing the single fracture experiment to an experiment utilizing the double fracture design. Figure 4 shows a sequence of CH_4 hydrate formation, CO_2 displacement, and CH_4–CO_2 exchange in a core plug with two parallel fractures. The MR signal in the fractures from the CH_4 gas (Image B) disappeared as CO_2 was injected and displaced the CH_4 gas from the fractures (Image C). Subsequently, the signal gradually reappeared as CO_2 exchanged with CH_4 and CH_4 gas diffused into the fractures (Image D).

It is assumed that CH_4 production is limited both by the kinetics of the exchange process and diffusion rates of CO_2 and CH_4. The objective of this experiment was therefore to identify which mechanism is dominating the exchange rate. A comparison of produced CH_4 at two different diffusion lengths (double fracture vs single fracture) is shown in Figure 5. Two similar experiments with respect to hydrate saturation (0.54–0.60 frac.), water saturation (0.02 frac.), and salinity (2.3–2.5 wt % NaCl) were chosen to isolate the effect of diffusion length. The production rates compare well for both CO_2 flushes in Figure 5, which indicates that diffusion (mass transport) is not the rate-limiting factor for the CH_4–CO_2 exchange reaction in these core plugs. However, three cautions are in order: (1) The slightly higher hydrate saturation for the double fracture experiment may impact the diffusion rate adversely. (2) For the double fracture experiment, N_2 was injected prior to the CO_2 injections to remove excess CH_4 gas. The goal was to exclude CH_4 produced from free CH_4 gas in the pore space. Consequently, the single fracture experiment has a higher initial CH_4 recovery rate than would be the case if the same procedure of pre-flushing had been conducted for both experiments. (3) The molar CH_4 concentration was lower in the double fracture experiment because the total fracture volume was larger than in the single fracture experiment. A direct comparison of molar CH_4 concentrations between the experiments is therefore difficult. Nonetheless, based on the similar initial rates for the two experiments, it seems like the dominant rate-limiting factor in these core-scale experiments is governed by the kinetics of the CH_4–CO_2 exchange process. Although much more surface area is provided within a porous medium compared to bulk samples, further access to CH_4 hydrate is limited when the outermost layer of CH_4 hydrate is converted to mixed CH_4–CO_2 hydrate. The critical question for CH_4–CO_2 exchange rate and ultimate recovery is then how much surface area is available for CO_2 to be exposed per volume CH_4 hydrate within the pores. This will be investigated in the following sections by comparing exchange rates for different CH_4 hydrates and water saturations.

3.3. Effect of Residual Water Saturation and Salinity.

An additional double fracture experiment with an initial water salinity of 3 wt % NaCl was conducted to investigate the effect of residual water saturation and salinity on the development of CH_4 gas recovery.[22] The brine salinity appeared to have a

https://dx.doi.org/10.1021/acs.energyfuels.0c03841
Energy Fuels 2021, 35, 2468–2477

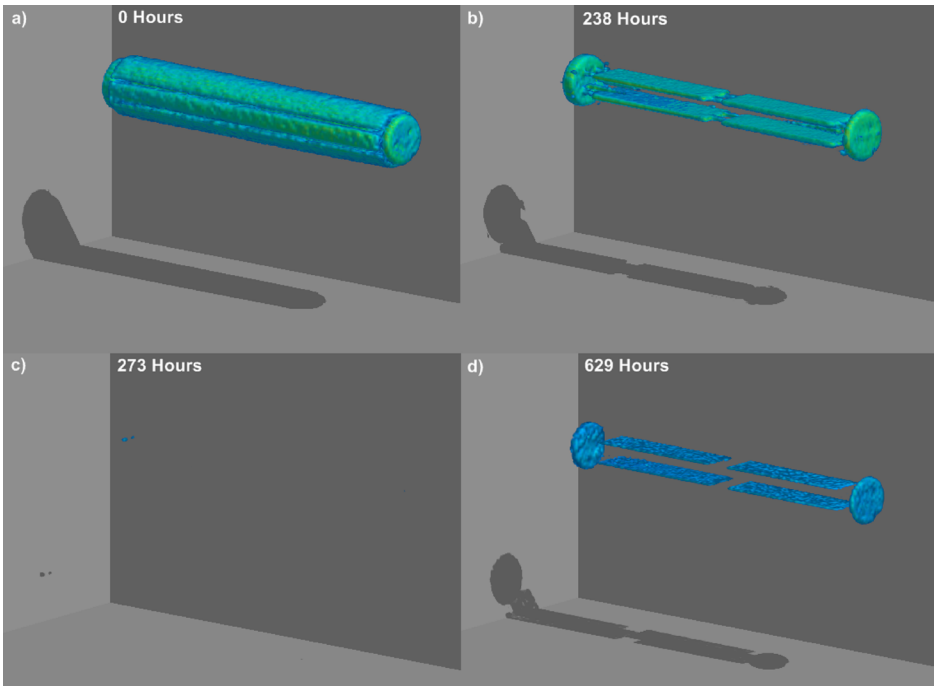

Figure 4. CH_4 gas produced by CO_2 replacement from a CH_4 hydrate-bearing core plug containing two fractures. The pore pressure was 8.3 MPa. (A) Before cooling with water and CH_4 gas in the pore space and CH_4 gas in the fractures. (B) After cooling (T = 4 °C) and hydrate formation with CH_4 hydrate in the pore space and CH_4 gas in the fractures. (C) After CO_2 flush with CH_4 hydrate in the pore space and CO_2 in the fractures. (D) CH_4 gas is produced back into the fractures by CO_2 replacement in the CH_4 hydrate.

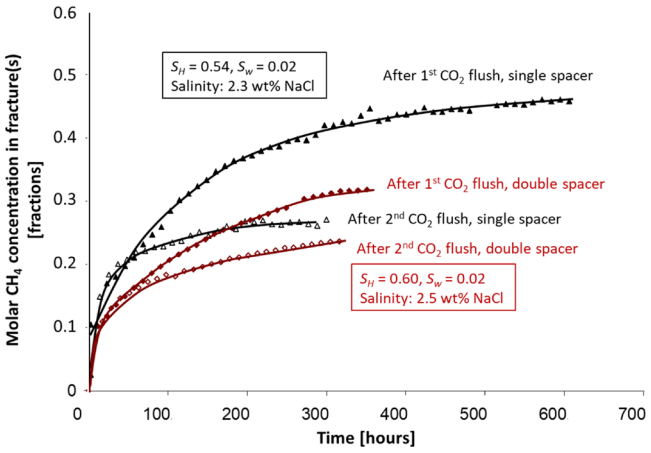

Figure 5. Molar CH_4 concentration in the fractures as deduced by average MR signals. The figure compares data from a single fracture experiment (black triangles) to a double fracture experiment (red diamonds). The pore pressure and temperature were 8.3 MPa and 4 °C, respectively. CH_4 hydrate formation was followed by a CO_2 flush to displace and produce CH_4 by CO_2 replacement. When CH_4 production ceased, a second CO_2 flush was conducted to increase the CO_2 concentration and thereby to increase the chemical potential. The molar CH_4 concentration was lower in the double fracture experiment because the total fracture volume was higher than in the single fracture experiment. Some of these results were also presented in Birkedal et al.[22] and Ersland et al.[25]

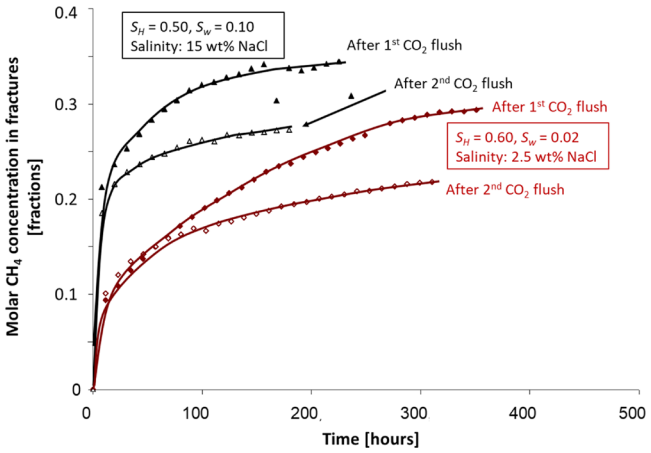

Figure 6. Molar CH_4 concentration in the fractures. The figure compares data from an experiment with low residual water saturation and salinity (red diamonds) to an experiment with high residual water saturation and salinity (black triangles). The pore pressure and temperature were 8.3 MPa and 4 °C, respectively. CH_4 hydrate formation was followed by a CO_2 flush to displace and produce CH_4 by CO_2 replacement. When CH_4 production ceased, a second CO_2 flush was conducted to increase the CO_2 concentration and thereby to increase the chemical potential. These results were also presented in Birkedal et al.[22]

positive impact on the CH_4 production rate; lower salinity and thereby less residual water saturation after CH_4 hydrate formation, decreased the initial rate and ultimate CH_4 gas recovery (Figure 6). The results corroborate models that predict higher conversion rates in the presence of residual liquid water.[26] The residual water provides transport channels for CO_2 diffusion along mineral grains and enhances the reaction surface area of the CH_4–CO_2 exchange process. However, the salinity of the residual water is of vital importance as CO_2 can form CO_2 hydrate with the pore water if the salinity is low. Formation of CO_2 hydrate from residual water will reduce the permeability of the porous medium severely and cause injectivity impairment. The formed CO_2 hydrate will shield and reduce the surface area of the CH_4

https://dx.doi.org/10.1021/acs.energyfuels.0c03841
Energy Fuels 2021, 35, 2468–2477

hydrate and limit the mass transfer. This adverse effect on the exchange reaction is shown in an experiment where the residual water saturation and salinity were 0.47 frac. and 5.5 wt % NaCl, respectively (Figure 7). Injection of nearly 0.9 pore

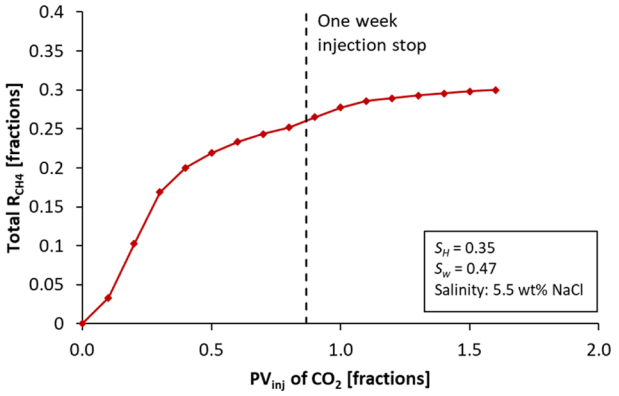

Figure 7. Total recovery of CH_4 gas as a function of pore volumes of CO_2 injected. The vertical dashed line represents a period of 1 week with no CO_2 injection, which allowed for diffusion and CH_4–CO_2 exchange to occur. The pore pressure and temperature were kept constant at 8.3 MPa and 4 °C, respectively, during the injection stop. CO_2 was injected with a constant volumetric flow rate of 1.2 mL/h before and after the injection stop.

volumes (PV) of CO_2 resulted in a total recovery of CH_4 gas equal to 0.25 frac. The constant flow rate injection was then stopped, and the pressure was kept constant at 8.3 MPa for 1 week to allow for diffusion of CO_2 from the fracture and into the core plug. However, the total recovery of CH_4 gas increased to only 0.3 frac. after additional 0.7 PV of CO_2 was injected with a constant flow rate after the injection stop. The amount of produced CH_4 gas was less than the amount of CH_4 originally present as free gas in the fracture and in the pore space.

3.4. Co-Current CO_2 Injection in Whole Cores. A series of displacement experiments where CO_2 was injected into CH_4 hydrate-saturated cores without fractures was conducted to mimic a production scenario with one injection well and one production well. Gas chromatography analysis of the produced effluent measured the fraction of CH_4 and CO_2. The experiments were prepared to study the impact of the following parameters: temperature, fluid saturations, N_2 content of the injectant, and alkanolamine injection (Table 1). The thermodynamic conditions for each experiment are summarized in Figure 8.

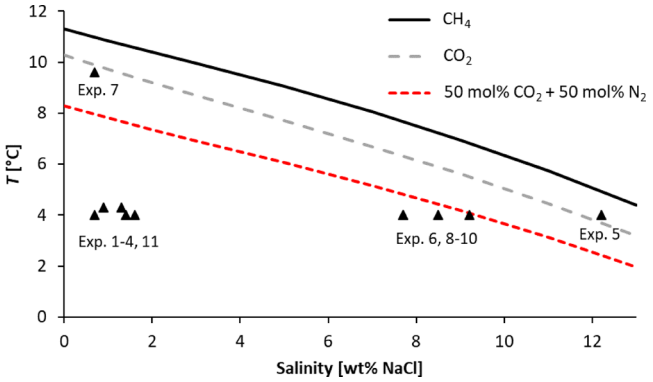

Figure 8. Thermodynamic conditions for displacement experiments in whole cores at P = 8.3 MPa. The hydrate equilibrium curves are calculated by the software PVTsim Nova.

3.5. Effect of Temperature. The rate and ultimate recovery of CH_4 gas increased as the exchange temperature increased (Figures 9 and 10). The ultimate recovery of CH_4

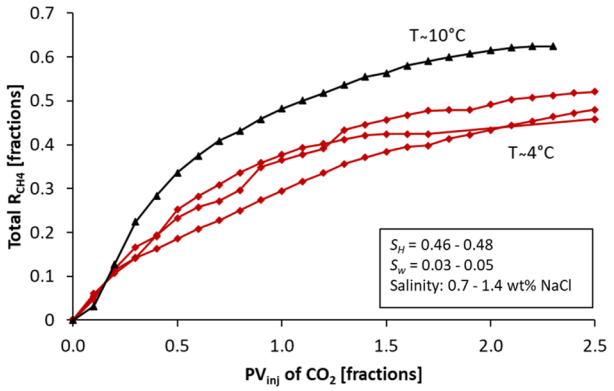

Figure 9. Total recovery of CH_4 gas as a function of pore volumes of CO_2 injected. The pore pressure was 8.3 MPa and CO_2 was injected with a constant volumetric flow rate of 1.2 mL/h. Exp. 7 (black triangles) was conducted at T = 9.6 °C while three duplicate experiments (Exp. 1, 2, and 4 in red diamonds) were conducted at T ≈ 4 °C.

gas (hydrate-bound CH_4 gas and free CH_4 gas) after injecting close to 2.5 PV of CO_2 was 0.1–0.2 frac. higher for 10 °C compared to 4 °C. The increased exchange temperature has several advantages promoting CH_4 gas production. At 10 °C, both CO_2 and CH_4 are closer to the dissociation temperature at P = 8.3 MPa compared to T = 4 °C. This means that the

Table 1. Overview of Displacement Experiments in Whole Cores at P = 8.3 MPa

exp.	injectant	T (°C) ±0.02	S_w (frac.) ±0.02	salinity (wt% NaCl)	S_H (frac.) ±0.02	S_{CH4} (frac.) ±0.02
1	CO_2	4.0	0.03	1.4	0.48	0.49
2	CO_2	4.3	0.03	1.3	0.48	0.49
3	CO_2	4.0	0.03	1.6	0.58	0.39
4	CO_2	4.3	0.05	0.9	0.46	0.49
5	CO_2	4.0	0.12	12.2	0.38	0.50
6	CO_2	4.0	0.29	7.7	0.46	0.25
7	CO_2	9.6	0.03	0.7	0.48	0.49
8	25% CO_2 + 75% N_2	4.0	0.27	8.5	0.51	0.22
9	40% CO_2 + 60% N_2	4.0	0.31	7.7	0.49	0.20
10	50% CO_2 + 50% N_2	4.0	0.24	9.2	0.49	0.27
11	50% CO_2 + 50% MEA	4.0	0.06	0.7	0.43	0.51

https://dx.doi.org/10.1021/acs.energyfuels.0c03841
Energy Fuels 2021, 35, 2468–2477

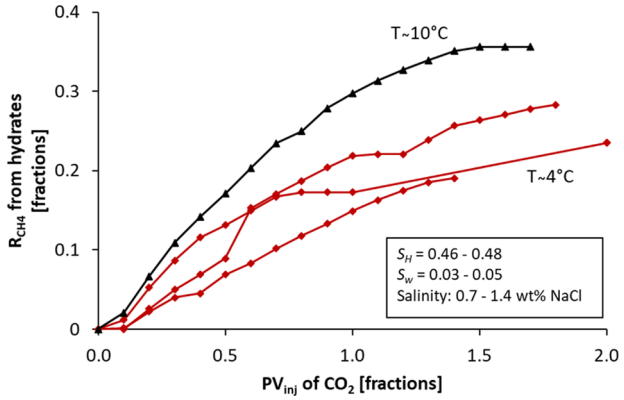

Figure 10. Recovery of hydrate-bound CH_4 gas as a function of pore volumes of CO_2 injected. Complete recovery of free CH_4 gas in the pore space is assumed before the recovery of hydrate-bound CH_4 gas starts. The pore pressure was 8.3 MPa and CO_2 was injected with a constant volumetric flow rate of 1.2 mL/h. Exp. 7 (black triangles) was conducted at T = 9.6 °C while three duplicate experiments (Exp. 1, 2, and 4 in red diamonds) were conducted at $T \approx 4$ °C.

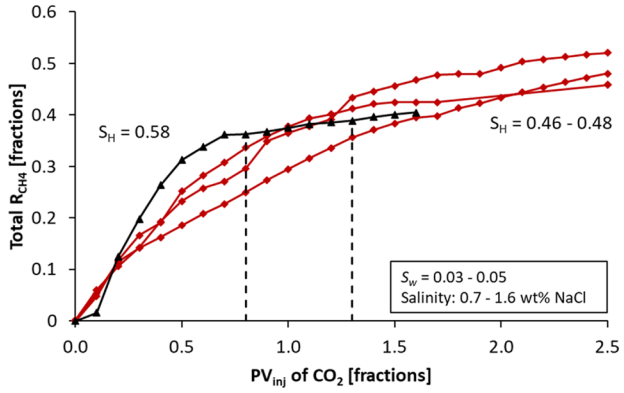

Figure 11. Total recovery of CH_4 gas as a function of pore volumes of CO_2 injected. The pore pressure and temperature were 8.3 MPa and 4 °C, respectively. CO_2 was injected with a constant volumetric flow rate of 1.2 mL/h for the duplicate experiments with low initial CH_4 hydrate saturation (Exp. 1, 2, and 4 in red diamonds), whereas the injection rate was 6.0 mL/h for the experiment with higher initial CH_4 hydrate saturation (Exp. 3 in black triangles). The vertical dashed lines represent periods of 12 h with no CO_2 injection in Exp. 3, which allowed for diffusion and CH_4−CO_2 exchange to occur.

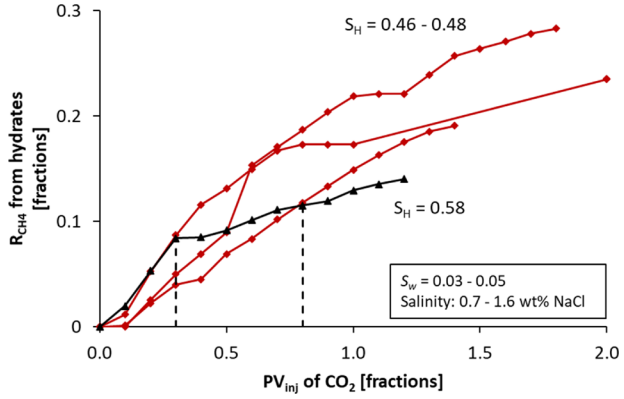

Figure 12. Recovery of hydrate-bound CH_4 gas as a function of pore volumes of CO_2 injected. Complete recovery of free CH_4 gas in the pore space is assumed before the recovery of hydrate-bound CH_4 gas starts. The pore pressure and temperature were 8.3 MPa and 4 °C, respectively. CO_2 was injected with a constant volumetric flow rate of 1.2 mL/h for the duplicate experiments with low initial CH_4 hydrate saturation (Exp. 1, 2, and 4 in red diamonds), whereas the injection rate was 6.0 mL/h for the experiment with higher initial CH_4 hydrate saturation (Exp. 3 in black triangles). The vertical dashed lines represent periods of 12 h with no CO_2 injection in Exp. 3, which allowed for diffusion and CH_4−CO_2 exchange to occur.

CH_4 hydrate is less stable at 10 °C and the CH_4 molecule is less bound by the hydrate cavity. The reduced driving force for CO_2 hydrate formation decreases the likelihood of extensive CO_2 hydrate growth with the pore water and thereby lowers the risk of permeability reduction and possible plugging. The increased temperature also enhances the diffusion rate constant. The increased CH_4 gas recovery with temperature is in line with previous experimental findings.[13,14,16] The CH_4 recovery increased substantially when the temperature was increased from 2 to 8 °C at P = 13 MPa.[14] This was explained by rapid CO_2 hydrate formation with the pore water at 2 °C, which reduced the permeability severely. At 8 °C, CO_2 hydrate formation was more moderate and the permeability reduction was local in discrete regions. The CO_2 flow diversion that followed resulted in an enhanced volumetric sweep efficiency and CO_2 contacted more of the CH_4 hydrate. When the temperature was increased further to 10 °C, which was outside of the CO_2 hydrate stability region, the recovery of CH_4 decreased again. Now, the authors argued that the initial dissociation of CH_4 hydrate formed preferential flow paths for the injected CO_2, which left most of the CH_4 hydrate uncontacted by CO_2.[14] Stanwix et al.[13] found that incremental thermal stimulation (−2 to 5 °C) at P = 3 MPa progressively enhanced the CH_4 recovery in quartz sediments.

3.6. Effect of CH_4 Hydrate Saturation. Increasing the CH_4 hydrate saturation seemed to have a negative effect on the ultimate recovery of CH_4 gas (Figures 11 and 12). The ultimate recovery of CH_4 gas was approximately 0.1 frac. higher for an initial CH_4 hydrate saturation of 0.46−0.48 compared to an initial CH_4 hydrate saturation of 0.58. It should be noted that the CO_2 injection was prolonged until 2.5 PV of CO_2 was injected for the duplicate experiments with an initial CH_4 hydrate saturation of 0.46−0.48, whereas only ∼1.5 PV of CO_2 was injected in the core plug with higher initial CH_4 hydrate saturation. However, the incremental CH_4 recovery between 0.5 and 1.5 PV of CO_2 injected was small for the high initial CH_4 hydrate saturation as compared with the experiments with lower initial CH_4 hydrate saturation (Figure 11). The rate of CH_4 gas recovery was on the contrary higher during the first 0.5 PV of CO_2 injected for the high initial CH_4 hydrate saturation case, but this was likely due to a higher volumetric injection rate of CO_2 (6.0 mL/h) there compared to the injection rate that was used for the lower CH_4 hydrate saturation experiments (1.2 mL/h). The high injection rate could invoke a better volumetric sweep of the free CH_4 gas in the core plug, which would give increased initial recovery. Most of the accessible free CH_4 gas was displaced early, while the hydrate-bound CH_4 gas produced by the CH_4−CO_2 exchange process was dominating the tail of the production. The recovery of hydrate-bound CH_4 gas was higher for lower initial CH_4 hydrate saturations (Figure 12). The exchange reaction is believed to proceed in a two-step process: A rapid surface reaction with partial dissociation followed by a slower solid diffusion reaction of guest molecules across the formed mixed hydrate layer.[27,28] When the initial CH_4 hydrate saturation was higher, the initial CH_4 gas saturation was

https://dx.doi.org/10.1021/acs.energyfuels.0c03841
Energy Fuels 2021, 35, 2468−2477

lower and below 0.4 frac., leaving CO_2 with less surface area to contact the CH_4 hydrate. A similar trend was observed by Masuda et al.[15] where the CH_4−CO_2 exchange recovery decreased from around 0.30 frac. at low CH_4 hydrate saturation to approximately 0.05 frac. at high CH_4 hydrate saturation.

3.7. Critical Residual Water Saturation. The diffusive CH_4−CO_2 exchange in fractured cores indicated that the existence of residual pore water promotes the CH_4−CO_2 exchange through liquid diffusion of CO_2 molecules in the water phase. The grain-wetting saline water films may then act as distribution channels for CO_2 to contact the CH_4 hydrate and thereby to increase the surface reaction area and the total exchange rate. This is clearly important for diffusion driven exchange experiments like the ones presented earlier with fractured core plugs. For flow experiments in whole core plugs, the residual water saturation is a critical parameter that highly affects the permeability of the core plug during CO_2 injection. CO_2 hydrate formation with the pore water is very effective in reducing the permeability and blocking the viscous flow of CO_2. It was not possible to sustain flow of CO_2 through the core plugs when the residual water saturation was above ∼0.1 frac. for CH_4 hydrate saturations in the interval of 0.38−0.58 frac. (Table 2). Notice that the average pore water salinity was below the stability salinity, which allowed for CO_2 hydrate formation with the residual pore water. Three attempts of injecting CO_2 into a core plug saturated with 0.46 frac. CH_4 hydrates and 0.29 frac. water is shown in Figure 13. The CO_2 injection was quickly terminated in the two first attempts as the injection pressure increased rapidly with no response in the outlet pressure. The injection pressure was set to 8.95 MPa after the third CO_2 injection and was maintained constant for 70 h to monitor the progression of the outlet pressure. The outlet pressure started to increase approximately 10 h after the injection pressure was set to 8.95 MPa and equalized the injection pressure after 50 h. The resistivity increased from 30 to 110 Ωm in the same period, indicating a substantial growth of CO_2 hydrate with the pore water. The permeability was therefore further reduced by the additional CO_2 hydrate formation and it was not possible to inject any CO_2 after this.

Table 2. Overview of Total Recovered CH_4 Gas by CO_2 Injection at P = 8.3 MPa and $T \approx 4$ °C

exp.	S_w (frac.) ±0.02	salinity (wt % NaCl)	S_H (frac.) ±0.02	S_{CH4} (frac.) ±0.02	total R_{CH4} (frac.)
1	0.03	1.4	0.48	0.49	0.52
2	0.03	1.3	0.48	0.49	0.46
3	0.03	1.6	0.58	0.39	0.40
4	0.05	0.9	0.46	0.49	0.49
5	0.12	12.2	0.38	0.50	plugged
6	0.29	7.7	0.46	0.25	plugged

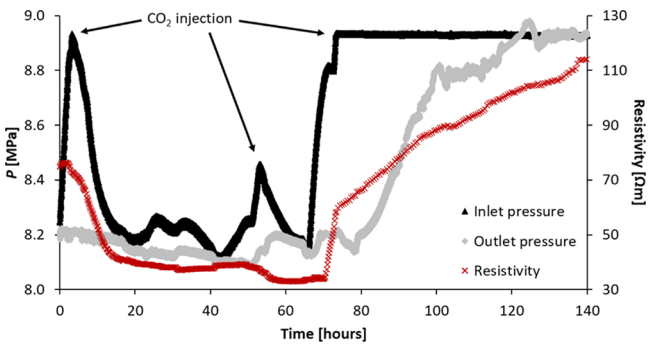

Figure 13. Development of differential pressure during three attempts of CO_2 injection at a constant volumetric flow rate of 60 mL/h in Exp. 6. The CH_4 hydrate saturation was 0.46 and the water saturation was 0.29 prior to CO_2 injection. The temperature was 4 °C.

3.8. Effect of N_2 in Co-Current CO_2 Injection. N_2 was co-injected with CO_2 to maintain injectivity and permeability in the core plugs at water saturations above 0.1 frac. Three different mixtures of N_2 and CO_2 were used to investigate the effect of N_2 content on CH_4 gas recovery in core plugs initially saturated with S_H = 0.49−0.51 frac. and S_w = 0.24−0.31 frac. (Figures 14 and 15). Injection of 25 mol % CO_2 and 75 mol %

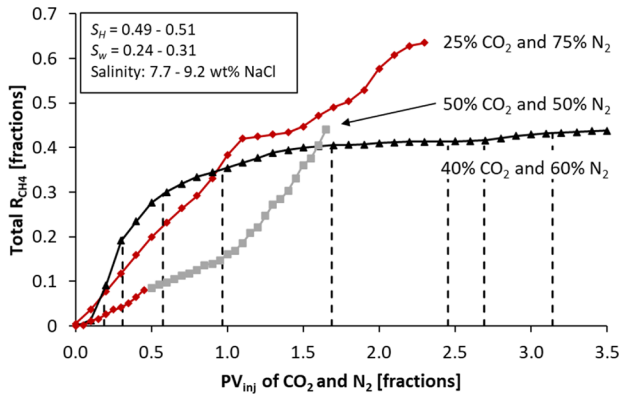

Figure 14. Total recovery of CH_4 gas as a function of pore volumes of CO_2 and N_2 injected. The pore pressure and temperature were 8.3 MPa and 4 °C, respectively. The mixture of N_2 and CO_2 was injected with a constant volumetric flow rate of 1.2 mL/h for two of the experiments (Exp. 8 in red diamonds and Exp. 10 in gray squares), whereas the injection rate was 2.0 mL/h when the injected CO_2 content was 40 mol % (Exp. 9 in black triangles). The vertical dashed lines represent periods of 12 h with no CO_2 injection in Exp. 9, which allowed for diffusion and CH_4−CO_2 exchange to occur.

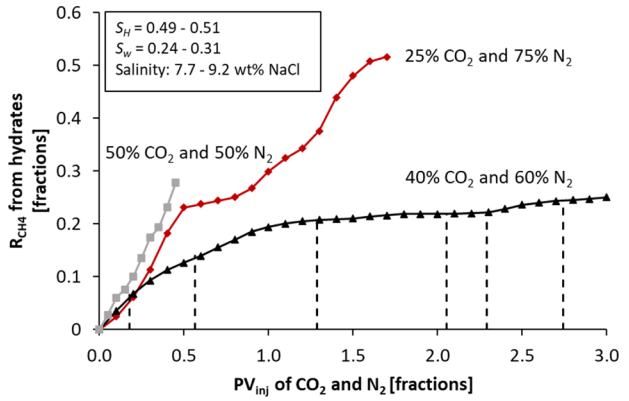

Figure 15. Recovery of hydrate-bound CH_4 gas as a function of pore volumes of N_2 and CO_2 injected. Complete recovery of free CH_4 gas in the pore space is assumed before the recovery of hydrate-bound CH_4 gas starts. The pore pressure and temperature were 8.3 MPa and 4 °C, respectively. The mixture of N_2 and CO_2 was injected with a constant volumetric flow rate of 1.2 mL/h for two of the experiments (Exp. 8 in red diamonds and Exp. 10 in gray squares), whereas the injection rate was 2.0 mL/h when the injected CO_2 content was 40 mol % (Exp. 9 in black triangles). The vertical dashed lines represent periods of 12 h with no CO_2 injection in Exp. 9, which allowed for diffusion and CH_4−CO_2 exchange to occur.

https://dx.doi.org/10.1021/acs.energyfuels.0c03841
Energy Fuels 2021, 35, 2468−2477

N_2 at a constant rate of 1.2 mL/h led to a total recovery of CH_4 gas above 0.6 frac., whereas injection of 40 mol % CO_2 and 60 mol % N_2 at a constant rate of 2 mL/h resulted in a total recovery of CH_4 gas of 0.4 frac. The effect of N_2 content on CH_4 gas recovery is highlighted in Exp. 10 where the injection mixture was changed during injection (Figure 14). Decreasing the concentration of N_2 from 75 to 50 mol % inflicted a temporary reduction of the rate of CH_4 gas recovery. However, as the injection of 50 mol % CO_2 and 50 mol % N_2 continued, the recovery rate of CH_4 gas improved and surpassed the recovery rates obtained by the other CO_2–N_2 mixtures (Figure 15). This highlights the advantage by injecting a thermodynamic inhibitor/destabilizing agent followed by pure CO_2 or high content CO_2 mixed with N_2, which will be further exemplified in the next section. Yasue et al.[17] obtained recovery rates of CH_4 gas from hydrate-bound CH_4 of 0.08–0.14 frac. when injecting a mixture of 59 mol % CO_2 and 41 mol % N_2 into hydrate-bearing cores with S_H = 0.48–0.54 frac. This matches the trend observed in Figure 15 where the recovery of CH_4 was 0.2 frac. for 40 mol % CO_2 and 0.5 frac. for 25 mol % CO_2. Cha et al.[11] measured a CH_4 recovery of 0.42 frac. when using a mixture of 20 mol % CO_2 and 80 mol % N_2 in an experiment with no flow. Simulation results indicated that the CH_4 recovery was maximized when the CO_2 content of the injectant was below 40 mol %.[17]

3.9. Effect of Alkanolamines in Co-Current CO_2 Injection. The effectiveness of injecting a hydrate inhibitor prior to CO_2 injection was investigated by using monoethanolamine (MEA) (Figures 16 and 17). MEA is a primary

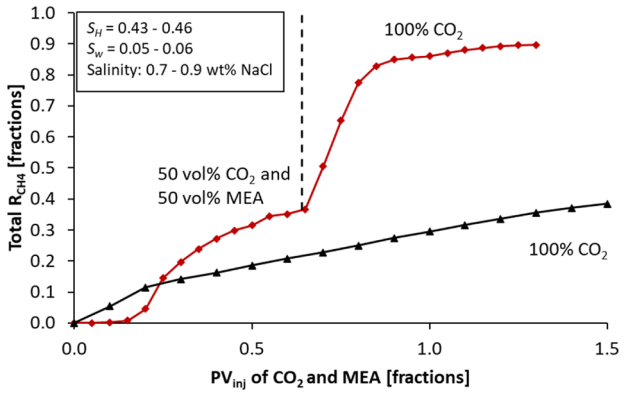

Figure 16. Total recovery of CH_4 gas as a function of pore volumes of CO_2 and MEA injected. The pore pressure and temperature were 8.3 MPa and 4 °C, respectively. The total volumetric flow rate was equal to 1.2 mL/h for both experiments (Exp. 11 in red diamonds and Exp. 4 in black triangles).

alkanolamine, which is soluble in water and will thus act as a hydrate inhibitor. MEA is also frequently used by the industry to remove CO_2 from exhaust gas.[29] The exothermic heat of reaction between MEA and CO_2 is ~84 kJ/mol,[30] which is larger than the endothermic heat absorbed during CH_4 hydrate dissociation (54.49 kJ/mol).[10] The motivation for adding MEA to the injected CO_2 was therefore to produce heat in the core plug, which would destabilize the CH_4 hydrate and aid the exchange process between CH_4 and CO_2. Injecting nearly 0.7 PV of 50 vol % CO_2 and 50 vol % MEA followed by pure CO_2 injection resulted in a total recovery of CH_4 gas of 0.9 frac. This is a substantial increase in total recovery and recovery rate as compared with pure CO_2 injection (Figure 16). The

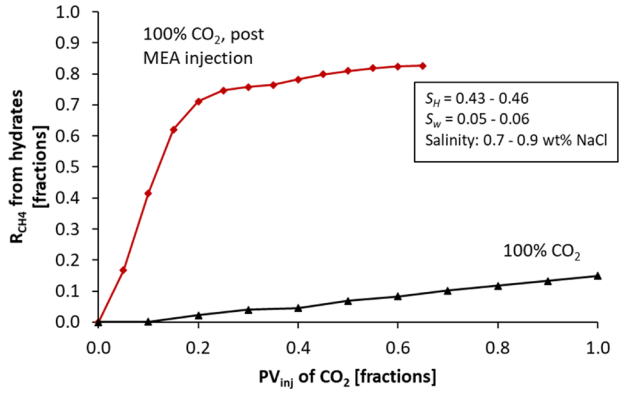

Figure 17. Recovery of hydrate-bound CH_4 gas as a function of pore volumes of MEA and CO_2 injected. Complete recovery of free CH_4 gas in the pore space is assumed before the recovery of hydrate-bound CH_4 gas starts. The pore pressure and temperature were 8.3 MPa and 4 °C, respectively. The total volumetric flow rate was equal to 1.2 mL/h for both experiments (Exp. 11 in red diamonds and Exp. 4 in black triangles).

exothermic reaction between MEA and CO_2 led to CH_4 hydrate dissociation inside the core plug, which was verified by liquid water production during the injection. More than 0.8 frac. of the hydrate-bound CH_4 was produced after injecting less than 1.5 PV of MEA and CO_2. The injection ratio of 50 vol % MEA was likely excessive, and lower doses of MEA should be tested to maximize the recovery rate of CH_4 gas while limiting the amount of produced liquid water. It should be noted that MEA is highly corrosive[31] and the environmental effect of potential degradation products from MEA is not clear.

3.10. Implications for Field-Scale Application. The results presented in this paper demonstrate the importance of the residual water saturation on the injectivity of CO_2 in CH_4 hydrate-bearing porous media. The injectivity of CO_2 became close to zero when the water saturation exceeded 0.1 frac. for CH_4 hydrate saturations in the interval of 0.38–0.58 frac. As most of the hydrate deposits that are targeted for CH_4 gas production consist of high hydrate saturations with the rest of the pore space saturated with water,[2,5,32] pure CO_2 injection is not recommended in these sediments. Neither is injecting pure CO_2 into hydrate accumulations found in permafrost-affected sediments as the CO_2 injectivity is low and the sub-zero temperature has an adverse effect on the exchange process. The recovery of CH_4 gas was highest when the exchange temperature was close to the hydrate equilibrium temperature. Injection of pure CO_2 is only an alternative in the special case where the hydrate reservoir contains free CH_4 gas originating from an underlying gas cap, which historically is referred to as a class 1G hydrate reservoir.[33]

Maintaining permeability that allows for efficient injection of fluids and production of CH_4 gas requires an injectant where the content of CO_2 is customized to the given CH_4 hydrate and water saturation of the reservoir. N_2 is an excellent candidate to mix with CO_2, which allows for efficient injectivity in hydrate-bearing core plugs with water saturations of at least 0.3 frac. The recovery of CH_4 gas is most effective when the content of N_2 is above 60 mol % for CH_4 hydrate saturations of ~0.5 frac. Injecting flue gas is therefore a viable option because of its typical composition of more than 65 mol % N_2 and less than 15 mol % CO_2.[34] Flue gas is readily available from power plants and is a low-cost alternative to acquiring

https://dx.doi.org/10.1021/acs.energyfuels.0c03841
Energy Fuels 2021, 35, 2468–2477

and mixing CO_2 with N_2. Co-injection of alkanolamines (specifically MEA) and CO_2 resulted in superior CH_4 gas recovery with more than 0.8 frac. of the hydrate-bound CH_4 produced after injecting less than 1.5 PV of MEA and CO_2. The best strategy on field scale would be to inject a limited slug of MEA before pure CO_2 injection. However, the use of alkanolamines incurs additional costs of acquisition and separation, as well as environmental effects, which must be investigated further.

The goal of this study was to elucidate processes and parameters that maximize the recovery of CH_4 gas by CH_4–CO_2 exchange in hydrate-bearing porous media. In addition to recovery rates, there are other concerns related to the exchange process that must be addressed considering the current situation with anthropogenic CO_2 emissions that lead to global warming. An important technology to reduce the CO_2 emissions is to implement carbon capture, utilization, and storage (CCUS). Using flue gas as the injectant is ideal in this matter as the cost of CO_2 capture is omitted. On the other hand, the content of CO_2 is low in flue gas and the amount of CO_2 which will be stored in the hydrate reservoir is limited. There is thus an incentive to increase the content of CO_2 in the injectant relative to N_2 to maximize the stored amount of CO_2. Future studies should aim to balance the need for injectivity and maximum CH_4 gas recovery with the potential for CO_2 sequestration. Additionally, the degree of CH_4 hydrate dissociation associated with the use of alkanolamines and elevated N_2 content must be addressed to investigate the geophysical integrity of the sediments during the recovery process. If the injection ultimately leads to large-scale dissociation of the CH_4 hydrate and water production, a simple pressure depletion process would instead be more cost-effective in dissociating the CH_4 hydrate and producing the CH_4 gas. The depleted hydrate reservoir can later be pressurized with concentrated flue gas to enable sequestration of CO_2. The principle of recover first and inject later does not require any CH_4 separation step, which lowers the expenses significantly.[35]

4. CONCLUSIONS

We have presented a series of experimental studies of CH_4–CO_2 exchange in CH_4 hydrate-bearing Bentheim sandstone core plugs at different experimental conditions. The following conclusions are drawn:

- The rate of CO_2–CH_4 exchange on core-scale seemed to be governed by CH_4–CO_2 exchange kinetics rather than diffusion length.
- The presence of residual water containing elevated salinity improved the initial rate and ultimate recovery of CH_4 gas in fractured core plugs. The residual water provided transport channels for CO_2 diffusion along mineral grains and enhanced the reaction surface area of the CH_4–CO_2 exchange process.
- Increasing the exchange temperature from 4 to 10 °C improved the initial rate and ultimate recovery of CH_4 gas at P = 8.3 MPa.
- The reduction of CO_2 injectivity was severe when the water saturation exceeded 0.1 frac. for CH_4 hydrate saturations in the interval of 0.38–0.58 frac. CO_2 hydrate formation with the residual pore water effectively decreased the permeability and blocked the core plug.
- Increased hydrate saturation (from 0.47 to 0.58 frac.) reduced the ultimate recovery of CH_4 gas due to mass transfer limitations and reduced surface area.
- The recovery of CH_4 gas was most effective when the content of N_2 was above 60 mol % (CO_2 < 40 mol %) for CH_4 hydrate saturations of ∼0.5 frac. and residual water saturations of ∼0.3 frac. Injection of flue gas may be a viable option in sediments containing elevated residual water saturations.
- Co-injection of 50 vol % MEA and 50 vol % CO_2 followed by pure CO_2 injection resulted in superior CH_4 gas recovery with more than 0.8 frac. of the hydrate-bound CH_4 produced after injecting less than 1.5 PV of MEA and CO_2.

AUTHOR INFORMATION

Corresponding Author

Stian Almenningen – *Department of Physics and Technology, University of Bergen, Bergen 5020, Norway*; orcid.org/0000-0002-2839-8503; Email: stian.almenningen@uib.no

Authors

Arne Graue – *Department of Physics and Technology, University of Bergen, Bergen 5020, Norway*

Geir Ersland – *Department of Physics and Technology, University of Bergen, Bergen 5020, Norway*

Complete contact information is available at: https://pubs.acs.org/10.1021/acs.energyfuels.0c03841

Notes

The authors declare no competing financial interest.

ACKNOWLEDGMENTS

The authors would like to acknowledge the invaluable contributions by Dr. Bjørn Kvamme, Dr. Knut Arne Birkedal, Dr. Jarle Husebø, Dr. James J. Howard, and Jim Stevens. The authors are also grateful for the work provided by several MSc students. A few of the experiments were performed in partnership with ConocoPhillips at the ConocoPhillips Technology Center (Bartlesville, OK, USA). Several of the authors are indebted to the Norwegian Research Council for funding.

REFERENCES

(1) Kvenvolden, K. A. Methane Hydrate - a major reservoir of carbon in the shallow geosphere? *Chem. Geol.* **1988**, *71*, 41–51.

(2) Konno, Y.; Fujii, T.; Sato, A.; Akamine, K.; Naiki, M.; Masuda, Y.; Yamamoto, K.; Nagao, J. Key Findings of the World's First Offshore Methane Hydrate Production Test off the Coast of Japan: Toward Future Commercial Production. *Energy Fuels* **2017**, *31*, 2607–2616.

(3) Li, J.-F.; Ye, J.-L.; Qin, X.-W.; Qiu, H.-J.; Wu, N.-Y.; Lu, H.-L.; Xie, W.-W.; Lu, J.-A.; Peng, F.; Xu, Z.-Q.; Lu, C.; Kuang, Z.-G.; Wei, J.-G.; Liang, Q.-Y.; Lu, H.-F.; Kou, B.-B. The first offshore natural gas hydrate production test in South China Sea. *China Geol.* **2018**, *1*, 5–16.

(4) Yamamoto, K.; Dallimore, S. Aurora-JOGMEC-NRCan Mallik 2006-2008 Gas Hydrate Research Project Progress. *Nat. Gas oil* **2008**, *304*, 285–4541.

(5) Boswell, R.; Schoderbek, D.; Collett, T. S.; Ohtsuki, S.; White, M.; Anderson, B. J. The Iġnik Sikumi Field Experiment, Alaska North Slope: Design, Operations, and Implications for CO_2–CH_4 Exchange in Gas Hydrate Reservoirs. *Energy Fuels* **2017**, *31*, 140–153.

(6) Graue, A.; Kvamme, B.; Baldwin, B.; Stevens, J.; Howard, J. J.; Aspenes, E.; Ersland, G.; Husebo, J.; Zornes, D. MRI Visualization of Spontaneous Methane Production From Hydrates in Sandstone Core Plugs When Exposed to CO2. *SPE J.* **2008**, *13*, 146−152.
(7) Jadhawar, P.; Yang, J.; Jadhawar, J.; Tohidi, B. *Preliminary Experimental Investigation on Replacing Methane in Hydrate Structure with Carbon Dioxide in Porous Media*; Fifth International conference on Gas Hydrates: Trondheim, Norway, 2005.
(8) Lee, H.; Seo, Y.; Seo, Y.-T.; Moudrakovski, I. L.; Ripmeester, J. A. Recovering Methane from Solid Methane Hydrate with Carbon Dioxide. *Angew. Chem.* **2003**, *115*, 5202−5205.
(9) Ota, M.; Morohashi, K.; Abe, Y.; Watanabe, M.; Smith, R. L., Jr.; Inomata, H., Jr. Replacement of CH_4 in the hydrate by use of liquid CO_2. *Energy Convers. Manage.* **2005**, *46*, 1680−1691.
(10) Goel, N. In situ methane hydrate dissociation with carbon dioxide sequestration: Current knowledge and issues. *J. Pet. Sci. Eng.* **2006**, *51*, 169−184.
(11) Cha, M.; Shin, K.; Lee, H.; Moudrakovski, I. L.; Ripmeester, J. A.; Seo, Y. Kinetics of Methane Hydrate Replacement with Carbon Dioxide and Nitrogen Gas Mixture Using in Situ NMR Spectroscopy. *Environ. Sci. Technol.* **2015**, *49*, 1964−1971.
(12) Espinoza, D. N.; Santamarina, J. C. P-wave monitoring of hydrate-bearing sand during CH_4−CO_2 replacement. *Int. J. Greenhouse Gas Control* **2011**, *5*, 1031−1038.
(13) Stanwix, P. L.; Rathnayake, N. M.; de Obanos, F. P. P.; Johns, M. L.; Aman, Z. M.; May, E. F. Characterising thermally controlled CH_4−CO_2 hydrate exchange in unconsolidated sediments. *Energy Environ. Sci.* **2018**, *11*, 1828−1840.
(14) Deusner, C.; Bigalke, N.; Kossel, E.; Haeckel, M. Methane Production from Gas Hydrate Deposits through Injection of Supercritical CO_2. *Energies* **2012**, *5*, 2112−2140.
(15) Masuda, Y.; Maruta, H.; Naganawa, S.; Amikawa, K.; Nagao, J.; Haneda, H.; Konno, Y. *Methane Recovery From Hydrate-Bearing Sediments By N2-CO2 Gas Mixture Injection: Experimental Investigation On CO2-CH4 Exchange Ratio*; Proceedings of the 7th International Conference on Gas Hydrates: Edinburgh, Scotland, UK, 2011.
(16) Tupsakhare, S. S.; Fitzgerald, G. C.; Castaldi, M. J. Thermally Assisted Dissociation of Methane Hydrates and the Impact of CO_2 Injection. *Ind. Eng. Chem. Res.* **2016**, *55*, 10465−10476.
(17) Yasue, M.; Masuda, Y.; Liang, Y. Estimation of Methane Recovery Efficiency from Methane Hydrate by the N_2−CO_2 Gas Mixture Injection Method. *Energy Fuels* **2020**, *34*, 5236−5250.
(18) Gauteplass, J.; Almenningen, S.; Ersland, G.; Barth, T. Hydrate seal formation during laboratory CO_2 injection in a cold aquifer. *Int. J. Greenh. Gas Control.* **2018**, *78*, 21−26.
(19) Park, Y.; Kim, D.-Y.; Lee, J.-W.; Huh, D.-G.; Park, K.-P.; Lee, J.; Lee, H. Sequestering carbon dioxide into complex structures of naturally occurring gas hydrates. *PNAS* **2006**, *103*, 12690−12694.
(20) Sun, Y.-F.; Zhong, J.-R.; Li, R.; Zhu, T.; Cao, X.-Y.; Chen, G.-J.; Wang, X.-H.; Yang, L.-Y.; Sun, C.-Y. Natural gas hydrate exploitation by CO_2/H_2 continuous Injection-Production mode. *Appl. Energy* **2018**, *226*, 10−21.
(21) Pandey, J. S.; Karantonidis, C.; Karcz, A. P.; von Solms, N. Enhanced CH_4-CO_2 Hydrate Swapping in the Presence of Low Dosage Methanol. *Energies* **2020**, *13*, 5238.
(22) Birkedal, K. A.; Hauge, L. P.; Graue, A.; Ersland, G. Transport Mechanisms for CO_2-CH_4 Exchange and Safe CO_2 Storage in Hydrate-Bearing Sandstone. *Energies* **2015**, *8*, 4073−4095.
(23) Baldwin, B. A.; Stevens, J.; Howard, J. J.; Graue, A.; Kvamme, B.; Aspenes, E.; Ersland, G.; Husebø, J.; Zornes, D. R. Using magnetic resonance imaging to monitor CH_4 hydrate formation and spontaneous conversion of CH_4 hydrate to CO_2 hydrate in porous media. *Magn. Reson. Imaging* **2009**, *27*, 720−726.
(24) Ersland, G.; Husebø, J.; Graue, A.; Baldwin, B. A.; Howard, J.; Stevens, J. Measuring gas hydrate formation and exchange with CO_2 in Bentheim sandstone using MRI tomography. *Chem. Eng. J.* **2010**, *158*, 25−31.
(25) Ersland, G.; Husebø, J.; Graue, A.; Kvamme, B. Transport and storage of CO_2 in natural gas hydrate reservoirs. *Energy Procedia* **2009**, *1*, 3477−3484.
(26) Kvamme, B.; Graue, A.; Buanes, T.; Kuznetsova, T.; Ersland, G. Storage of CO_2 in natural gas hydrate reservoirs and the effect of hydrate as an extra sealing in cold aquifers. *Int. J. Greenhouse Gas Control* **2007**, *1*, 236−246.
(27) Falenty, A.; Qin, J.; Salamatin, A. N.; Yang, L.; Kuhs, W. F. Fluid Composition and Kinetics of the in Situ Replacement in CH_4−CO_2 Hydrate System. *J. Phys. Chem. C* **2016**, *120*, 27159−27172.
(28) Zhao, J.; Zhang, L.; Chen, X.; Fu, Z.; Liu, Y.; Song, Y. Experimental Study of Conditions for Methane Hydrate Productivity by the CO_2 Swap Method. *Energy Fuels* **2015**, *29*, 6887−6895.
(29) McCann, N.; Phan, D.; Wang, X.; Conway, W.; Burns, R.; Attalla, M.; Puxty, G.; Maeder, M. Kinetics and Mechanism of Carbamate Formation from CO_2(aq), Carbonate Species, and Monoethanolamine in Aqueous Solution. *J. Phys. Chem. A* **2009**, *113*, 5022−5029.
(30) Vaidya, P. D.; Mahajani, V. V. Quickly design CO_2 - amine absorber. *Indian J. Chem. Technol.* **2006**, *13*, 47−52.
(31) Xie, N.; Chen, B.; Tan, C.; Liu, Z. Energy Consumption and Exergy Analysis of MEA-Based and Hydrate-Based CO_2 Separation. *Ind. Eng. Chem. Res.* **2017**, *56*, 15094−15101.
(32) Collett, T. S.; Boswell, R.; Waite, W. F.; Kumar, P.; Roy, S. K.; Chopra, K.; Singh, S. K.; Yamada, Y.; Tenma, N.; Pohlman, J.; Zyrianova, M. India National Gas Hydrate Program Expedition 02 Summary of Scientific Results: Gas hydrate systems along the eastern continental margin of India. *Mar. Pet. Geol.* **2019**, *108*, 39−142.
(33) Moridis, G. J.; Kowalsky, M. B.; Pruess, K. Depressurization-Induced Gas Production From Class-1 Hydrate Deposits. *SPE Reservoir Eval. Eng.* **2007**, *10*, 458−481.
(34) Song, C.; Pan, W.; Srimat, S. T.; Zheng, J.; Li, Y.; Wang, Y.-H.; Xu, B.-Q.; Zhu, Q.-M. *Tri-reforming of Methane over Ni Catalysts for CO2 Conversion to Syngas With Desired H2/CO Ratios Using Flue Gas of Power Plants Without CO2 Separation*; Park, S.-E.; Chang, J.-S; Lee, K.-W., Eds.; Elsevier: 2004; 315−322.
(35) Englezos, P. Extraction of methane hydrate energy by carbon dioxide injection-key challenges and a paradigm shift. *Chin. J. Chem. Eng.* **2019**, *27*, 2044−2048.

https://dx.doi.org/10.1021/acs.energyfuels.0c03841
Energy Fuels 2021, 35, 2468−2477